Delamination growth analysis in composite laminates subjected to low velocity impact

Masoud Kharazan [*1], M.H. Sadr [1a] and Morteza Kiani [2,3b]

[1] *Aerospace Engineering Department & Center of Excellence in Computational Aerospace Engineering, Amirkabir University of Technology, Tehran, Iran*
[2] *Center for Advanced Vehicular Systems, Mississippi State University, Starkville, Mississippi, USA*
[3] *Engineering Technology Associate (ETA), Troy, MI 48083, USA*

Abstract. This paper presents a high accuracy Finite Element approach for delamination modelling in laminated composite structures. This approach uses multi-layered shell element and cohesive zone modelling to handle the mechanical properties and damages characteristics of a laminated composite plate under low velocity impact. Both intralaminar and interlaminar failure modes, which are usually observed in laminated composite materials under impact loading, were addressed. The detail of modelling, energy absorption mechanisms, and comparison of simulation results with experimental test data were discussed in detail. The presented approach was applied for various models and simulation time was found remarkably inexpensive. In addition, the results were found to be in good agreement with the corresponding results of experimental data. Considering simulation time and results accuracy, this approach addresses an efficient technique for delamination modelling, and it could be followed by other researchers for damage analysis of laminated composite material structures subjected to dynamic impact loading.

Keywords: composite materials; intralaminar damage; interlaminar damage; delamination; cohesive zone modelling; impact loading

1. Introduction

A wide range of fibre-reinforced composite materials are used in aerospace and automotive industries due to relatively low weight in combination with high specific stiffness and strength compared to metallic alloys. For example, more than 50% of the primary structure in Boeing 787 has been made of composite materials such as carbon fibre or sandwich panels, and the design of this airplane will be probably followed soon by Airbus A350 (Jackson *et al.* 2012). However the damage of composite materials under impacting by foreign objects is one of the great concerns of their applications since the impact-induced damages can significantly reduce strength and fatigue life of composite material structures.

∗Corresponding author, M.Sc., E-mail: Kharazan@aut.ac.ir
[a] Professor, Email: Sadr@aut.ac.ir
[b] Ph.D., E-mail: Mkiani@eta.com

Low velocity impact of laminated composite is the main factor that limits widespread application of this branch of materials especially in aerospace and automotive industries. Impact loads can result different forms of damages in laminated composite structures. These damages are classically divided in two main categories.

The first category is identified as intralaminar damages which developing inside plies such as matrix cracking and fibre breakage. The second category is addressed as interlaminar damages which develop at the interface between two adjacent plies, called delamination. Many researchers have experimentally studied composite material structures under impact loading (Davies and Zhang 1995, Abrate 1998, Reid and Zhou 2000, Davies and Zhang 2004) and few analytical solutions have been proposed based on simplifying the problem (Zheng 2007). These approaches often result errors due to oversimplification; consequently, these errors limit the application of the analytical approaches in damage analysis for composite material subjected to low velocity impact.

By improving computational performance in the last decade, various finite element (FE) approaches have been introduced to model the damages developed by impact loading. Wang *et al.* (2013), Aymerich *et al.* (2008), Finn and Springer (1993), Kim *et al.* (2013), Zhou *et al.*(2013) and Hosseini-Toudeshky *et al.* (2013) have studied different kinds of composite structures, either laminated or sandwich panels under various loading. These researchers used simulation techniques to investigate modelling of delamination by application of shell, solid, or hybrid shell-solid elements; however, the advantages and disadvantages of each FE modelling approach are still under discussion in literature (Dogan *et al.* 2012). From the viewpoint of industrial application to design composite structures by FE approach, where the structures are mostly thin, implementation of shell elements is highly suggested over solid or hybrid models. This can be explained by considering the complexity and number of elements necessary for modelling a thin structure through solid or shell elements. If solid elements are used to model a thin structure, the complexity and number of necessary elements for the model extensively increases. Consequently, shell elements are highly preferred.

Today, the major commercial software that can be used in crash simulations include: LS-DYNA, ABAQUS Explicit, PAM-CRASH, DYTRAN, and RADIOSS. Many of researchers such as (Maio *et al.* 2013, Heimbs *et al.* 2009, Feraboli *et al.* 2011) used LS-DYNA to simulate the impact response of structures made of different composite materials. Maio *et al.* (2013) deals with the prediction of the delamination damage induced by low velocity impact in a laminated composite plate using progressive damage model (MAT162) implemented in LS-DYNA and achieved acceptable results for shape and orientation of the observed delamination. However lots of efforts and investigations are still necessary for improvement damage modelling in composite laminates under impact loading. These investigations help to achieve comprehensive information for energy absorption mechanisms, failures modes, and residual mechanical strength of composite material structures that are needed for improvement the performance of composite structures (Kiani *et al.* 2013).

This paper presents a significant approach for delamination growth analysis in the laminated composite structures by application of shell elements and cohesive-zone modelling. The procedures and advantages of the current approach are discussed in detail and results are compared to the experiment presented in the literature (Choi and Chang 1992). In addition, the energy absorption mechanisms for laminated composite materials under low velocity impact are discussed.
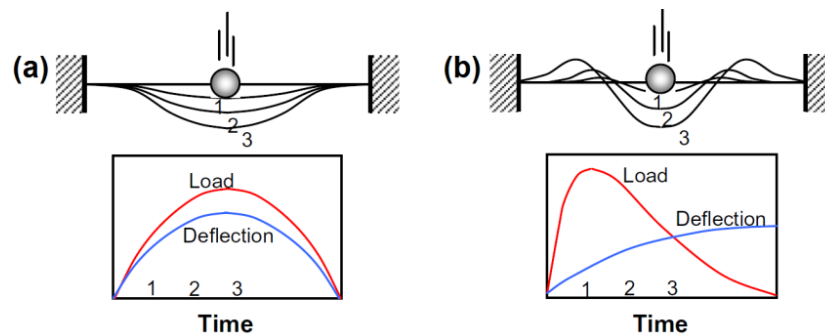
Fig. 1 Comparison between (a) large-mass and (b) small-mass impact (Olsson 2003)

2. Low velocity impact phenomenon

Impact on structures is often classified in two main categories as low-velocity and high-velocity impacts. However, a similar classification is proposed as boundary controlled and wave controlled impacts which are associated with the response of the structure to large-mass and small-mass impactors. A mass-ratio criterion governing the boundary controlled and wave controlled impact responses has been derived in detail by Olsson (2003). Olsson shows that wave controlled impact occurs when the mass of impactor is less than one quarter of the mass of the structure, which waves do not interfere with the boundaries. It is clear that when a structure is impacted, the elastic waves propagate throughout in the structure from the impact point.

Impact response of a structure is related to the impact duration. If the impact duration is in order of transition time for dilatational waves, response of the structure is dominated by dilatational waves. In addition, when the impact duration is longer than the time for the waves to reach the boundaries of the structure, the response can be studied under quasi-static consideration. On the other hand, impact velocity is the major parameter that alters the impact response for composite material structures; therefore, most of the impact responses are investigated under low and high velocity impact categories. However, an intermediate impact velocity can be considered between low-velocity and high-velocity impact events.

Different damages that propagate in a structure can change the structural impact responses especially for composite materials. Indeed, the impact response of a laminated composite structure is a very complicated phenomenon that is dominated by the interaction of two main categories of the damage. These two categories of damage and their interaction (Fig. 2) are classically explained as follows:

- The intralaminar failures, such as damages developing in each ply like matrix cracking, fibre breakage and fibre matrix debonding
- The interlaminar failures, such as damages developing in each ply interface between two adjacent ply which called delamination.

In low velocity impact phenomenon, matrix cracks are developed by tensile, compressive and shear stresses, and usually the cracks distribute within the entire damage region. Fibre compressive and shear failure are observed locally in contact region, while the local fibre tensile failure typically develops on the opposite surface and in the area including the large matrix cracks.
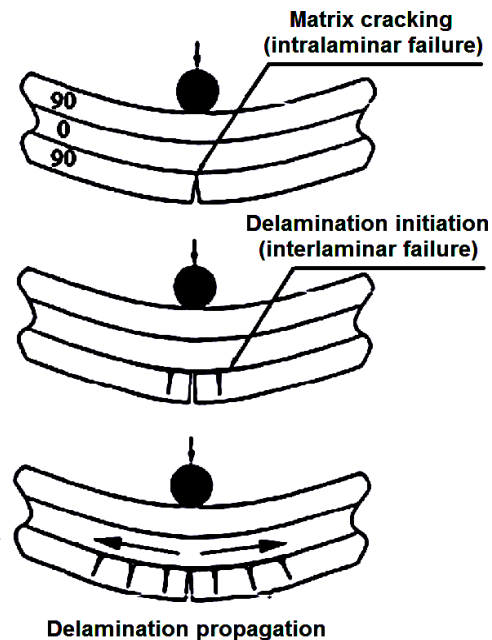
Fig. 2 Diagram of the principle of interaction between intralaminar and interlaminar damage of laminated composite (Chang and Chang 1992)

Delamination is particularly serious failure in the laminar structures because it forms at relatively low contact loads and plays important role in the flexural stiffness and buckling failure. Different orientations of the plies within a laminate can intensify the delamination for two adjacent plies due to the mismatch stiffness at their interface.

The delamination areas are influenced directly by the change in the impact energy. A typical distribution of delamination due to impact is shown by Fig. 3. At the interfaces between plies with different fibre orientations, the delamination is usually observed as "peanut shaped" with their major axis oriented in the direction of the fibres at the lower ply (Zheng 2007).
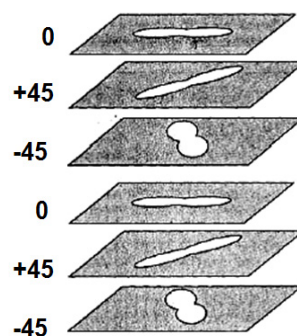

Fig. 3 Shapes of impact-induced delaminations (Abrate 1998)

3. Theory and background

This study focuses on development an approach that efficiently predicts delamination in a laminated composite panel under low velocity impact with high degree of accuracy and inexpensive simulation time. Because of small thickness to length ratio of the panel and negligible stress in the thickness direction, a 2D modelling with shell approach is suggested. As discussed before, application of shell elements instead of 3D solid elements can significantly reduce the simulation time and somehow increase the accuracy and performance for the FE approach. Following sections explain the two important damage classes in composite materials.

3.1 Intralaminar failure modelling

To model laminated composite plate and considering of intralaminar failures, LS-DYNA explicit code is used in this study because of large different contact algorithms and various material models implemented in this software. Many literatures reported a good capability of Enhanced-Composite-Damage (MAT54) material model in LS-DYNA for composite material analysis (Feraboli *et al.* 2011, Kiani *et al.* 2013); therefore, this material model was selected for the current study. Note should be taken that MAT54 is only valid for shell element modelling approach and it has been implemented based on the failure criteria developed by Chang and Chang (1987).

In the elastic region, stress-strain behaviour of the material for fibre (axial, 1 direction), matrix (transverse, 2 direction) and shear (12 direction) are given by following equations (Wade and Feraboli 2012)

$$\varepsilon_1 = \frac{1}{E_1}\left(\sigma_1 - v_{12}\sigma_2\right) \tag{1}$$

$$\varepsilon_2 = \frac{1}{E_2}\left(\sigma_2 - v_{21}\sigma_1\right) \tag{2}$$

$$2\varepsilon_{12} = \frac{1}{G_{12}}\tau_{12} + \alpha\tau_{12}^3 \tag{3}$$

where σ and ε are stresses and strains for the mentioned direction, τ_{12} is the shear stress, E_1 and E_2 are the young's modulus in longitudinal and transverse directions, G_{12} is shear modulus and α in Eq. (3) is a weighting factor for nonlinear shear stress term.

Beyond the elastic region, damage occurs when one or more criteria defined by the Chang/Chang formulation are satisfied. In these four criteria, a special criterion for shear stresses is not defined but the interaction of shear stresses is included in the failure criteria by using parameter β in the formulation. It is worth noting that the matrix tensile failure plays the most important role in the low velocity impact phenomenon; therefore, the material model must consider the failure in the matrix direction. The Chang/Chang material model in LS-DYNA includes typical damage criteria for unidirectional and fabric composite materials in all material directions which can be demonstrated as follows (LS-DYNA 2012, Schweizerhof *et al.* 1998):

- For tensile fibre failure mode where $\sigma_1 \geq 0$

$$e_f^2 = \left(\frac{\sigma_1}{X_t}\right)^2 + \beta\left(\frac{\tau_{12}}{S_c}\right)^2 - 1 \begin{cases} \geq 0 & \text{failed} \\ < 0 & \text{elastic} \end{cases} \tag{4}$$

After failure $E_1 = E_2 = G_{12} = v_{12} = v_{21} = 0$
- For compressive fibre failure mode where $\sigma_1 < 0$

$$e_c^2 = \left(\frac{\sigma_1}{X_c}\right)^2 - 1 \begin{cases} \geq 0 & \text{failed} \\ < 0 & \text{elastic} \end{cases} \tag{5}$$

After failure $E_1 = v_{12} = v_{21} = 0$
- For tensile matrix failure mode where $\sigma_2 \geq 0$

$$e_m^2 = \left(\frac{\sigma_2}{Y_t}\right)^2 + \left(\frac{\tau_{12}}{S_c}\right)^2 - 1 \begin{cases} \geq 0 & \text{failed} \\ < 0 & \text{elastic} \end{cases} \tag{6}$$

After failure $E_2 = v_{21} = G_{12} = 0$
- For Compressive matrix failure mode where $\sigma_2 < 0$

$$e_d^2 = \left(\frac{\sigma_2}{2S_c}\right)^2 + \left[\left(\frac{Y_c}{2S_c}\right)^2 - 1\right]\left(\frac{\sigma_2}{Y_c}\right) - \left(\frac{\tau_{12}}{S_c}\right)^2 - 1 \begin{cases} \geq 0 & \text{failed} \\ < 0 & \text{elastic} \end{cases} \tag{7}$$

After failure $E_2 = v_{21} = v_{21} = G_{12} = 0$
where X_t is the strength value for fibre tensile, X_c is the strength value for fibre compressive, Y_t is the strength value for matrix tensile, Y_c is the strength value for matrix compressive and S_c is the shear strength value of the unidirectional ply. Whenever one or more criteria defined by Eqs. (4)-(7) are satisfied in a ply within the element, the elastic properties for that ply are set to zero, and consequently if all the plies within an element fail, then the element will be considered as the failed element and removed from the FE simulation.
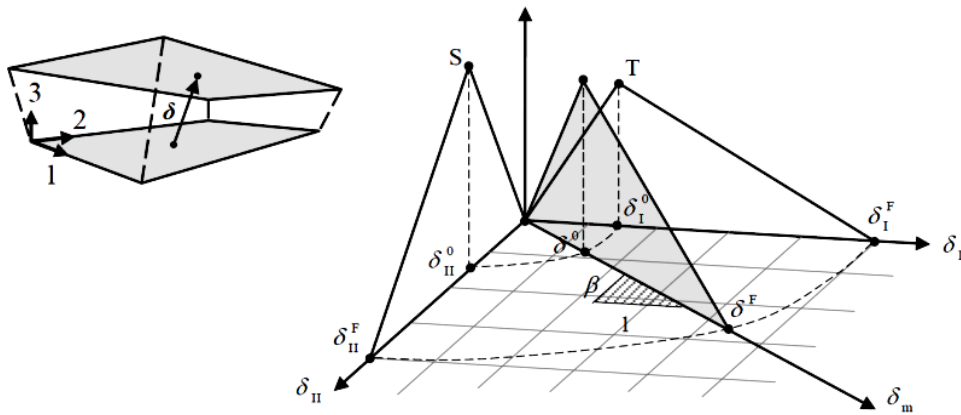

Fig. 4 Mix mode traction-separation law (LS-DYNA 2012)

3.2 Interlaminar failure modelling

Interlaminar failure (delamination) plays a significant role in low velocity impact for composite plates because of altering the energy absorption mechanism and degrading factor of the plate's stiffness.

To investigate the delamination propagation at interfaces in laminated composite, an extension of Dycoss Discrete Crack model is used. This extension is defined based on a bilinear traction-separation cohesive law with quadratic mixed mode delamination criterion and a damage formulation. This extension defines a fracture model based on cohesive material model MAT138 (MAT_COHESIVE_MIXED_MODE) which is used with a bilinear traction-separation law as shown in Fig. 4.

In this cohesive model, the ultimate displacements in both normal and tangential directions are equal to the displacement at the time when the cohesive contact fails completely. Moreover, a linear stiffness for loading, which is followed by linear softening during the damage, defines an accurate but simple relationship between the ultimate displacement and peak tractions as well as the energy release rate (LS-DYNA 2012)

$$G_{Ic} = \frac{1}{2} T \times \delta_{If} \tag{8}$$

$$G_{IIc} = \frac{1}{2} S \times \delta_{IIf} \tag{9}$$

where G_{IC} and G_{IIc} are the energy release rates for normal and shear interface failure, T and S are the peak tractions in normal and tangential directions.

In this cohesive zone model, the total mixed-mode relative displacement δ_m is defined as $\delta_m = \sqrt{\delta_I^2 + \delta_{II}^2}$, where $\delta_I = \delta_3$ is separation in normal direction, and $\delta_{II} = \sqrt{\delta_1^2 + \delta_2^2}$ is separation in tangential direction. The mixed-mode displacement for damage initiation δ^0 is given by following equation (LS-DYNA 2012)

$$\delta^0 = \delta_I^0 \delta_{II}^0 \sqrt{\frac{1+\beta^2}{(\delta_{II}^0)^2 + (\beta\delta_I^0)^2}} \tag{10}$$

where $\delta_I^0 = \dfrac{T}{K_N}$ and $\delta_{II}^0 = \dfrac{S}{K_T}$ are damage initiation separations in single modes, $\beta = \dfrac{\delta_{II}}{\delta_I}$ is mode mixity which is shown in Fig. 4, and the K_N and K_T are normal and tangential stiffness of the cohesive zone. The final mixed-mode separation for the power law ($\alpha > 0$) and for Benzeggagh-Kenane law ($\alpha < 0$) (Benzeggagh and Kenane 1996) are given by

$$\delta^F = \frac{2(1+\beta)^2}{\delta^0}\left[\left(\frac{K_N}{G_{Ic}}\right)^\alpha + \left(\frac{K_T.\beta^2}{G_{IIc}}\right)^\alpha\right]^{-\frac{1}{\alpha}} \quad \text{for} \quad \alpha > 0 \tag{11}$$

$$\delta^F = \frac{2}{\delta^0\left(\dfrac{1}{1+\beta^2}K_N + \dfrac{\beta^2}{1+\beta^2}K_T\right)}\left[G_{Ic} + (G_{IIc} - G_{Ic})\left(\frac{\beta^2.K_T}{K_N + \beta^2.K_T}\right)^{|\alpha|}\right] \quad \text{for} \quad \alpha < 0 \tag{12}$$

For the cohesive zone model used in this study, the damage of the interfaces is addressed by unloading paths from loading and softening paths where the unloading path is pointing to the origin. Fig. 5 shows a cohesive zone which is modelled between two multilayers shell elements by using contact definition.

4. FE modelling approach

In this paper, a low velocity impact on a rectangular T300/976 graphite/epoxy plate with clamped minor edges was studied for two different layup configurations, and the ply orientations as well as the configurations for each specimen used in the investigation are shown in Table 1. In addition, the transient impact response of both specimens was investigated under following assumptions:

- No friction between spherical impactor and laminated plate
- Impactor assume as rigid body
- Neglecting the damping effect in laminated structure
- Skip of considering the gravity force during impact.

Numerical simulation of delamination were carried out by using tie-break contact (*CONTACT_AUTOMATIC_ONEWAY_SURFACE_TO_SURFACE_TIEBREAK) with contact OPTION = 11 which is based on bilinear traction-separation law that was mentioned in the last section. Tiebreak contact allows the transmission of both tensile and compressive forces. The separation of the slave node from the master is resisted by a contact spring until failure, after which the tensile coupling is removed. The BREAK part of the contact allows modelling of failure where the spring decouples tensile forces, allowing independent motion of the slave node under tension. Post failure in all TIEBREAK contacts allows nodes to interact with segments as in traditional compression only contacts.

Table 2 shows the necessary material properties for the composite material used in this study (Choi and Chang 1992, Hosseini-Toudeshky 2006)

Table 1 Ply orientations and geometries of the specimens

Specimens	Ply orientation	Thickness	Span length	Width
S1	$[0_3 / 90_3 / 0_3 / 90_3 / 0_3]$	2.16 mm	100 mm	76 mm
S2	$[45_4 / -45_8 / 45_4]$	2.30 mm	100 mm	76 mm

Table 2 Mechanical properties for the laminated composite material

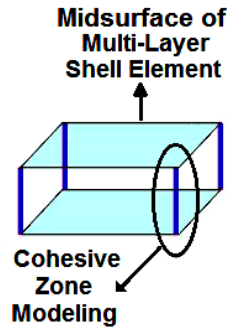| E_{11} (GPa)	E_{22} (GPa)	E_{33} (GPa)	G_{12} (GPa)	G_{23} (GPa)	G_{13}(GPa)
156.00	9.09	9.09	6.96	3.24	6.96
ρ (kg/m^3)	v_{12}	v_{13}	v_{23}	G_{Ic} (J/m^2)	G_{IIc} (J/m^2)
1540	0.228	0.228	0.40	157.0	350.0
X_t (MPa)	X_c (MPa)	Y_t (MPa)	Y_c (MPa)	S_{12} (MPa)	
1520.0	1590.0	45.0	252.0	105.0	

Fig. 5 Cohesive zone modelled between multi-layered shell element (one integration point for each single ply)
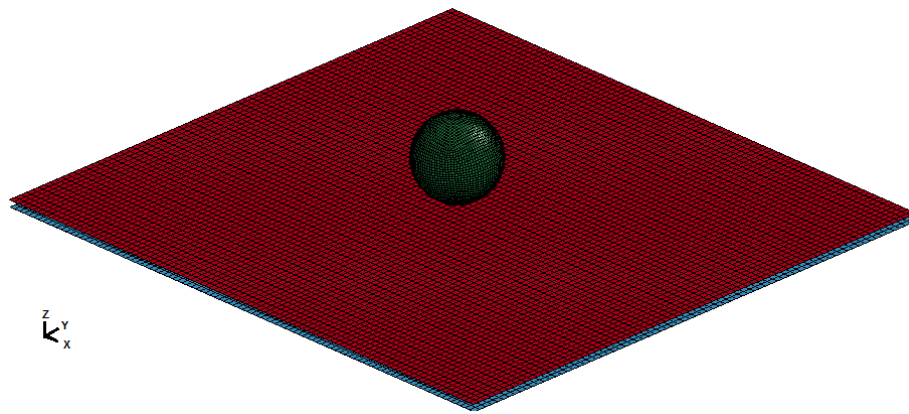

Fig. 6 FE model of the laminated plate and impactor

The impactor was considered as a spherical rigid body made of steel with nominal radius of 6.35 mm and mass of 0.16 kg which is travelled with initial velocity of 3 to 6 m/s for different test cases. The laminated plate was modelled by using two offset shell elements in thickness and one cohesive zone between them (lower 0/90 and 45/-45 interfaces). Inside each shell element a number of sub-layers have been defined in the shell thickness direction which represents the laminate layup by using one integration point for each single ply. This modelling approach referred as "layered shell" (Heimbs *et al.* 2009).

For modelling delamination in a laminated composite structure, one cohesive interface is used. Based on the different cases investigated in this study, when more than one cohesive interface is used in the model, bending stiffness of the model is reduced significantly, even no delamination occurs. On the other hand, bending stiffness for a stacked shell model is reduced by increasing the number of delamination contact layers.

The laminated plate in this study was modelled by using two offset shell elements through the thickness and one cohesive zone between them (lower 0/90 and 45/-45 interfaces). This offset distance is equal to one half of the upper shell thickness plus one half of the lower shell thickness.

To obtain better performance for the shell element application, Belytschko-Tsay element formulation (ELFORM 2) was used in the FE modelling which can provide a stiffness hourglass

controlling for the elements (LS-DYNA 2012, Belytschko 1984). The mesh size for the model was considered as 1 mm which is relatively defined based on the thickness of the plate. This consideration resulted number of 18,950 elements and 19,306 nodes in the FE model. The spherical impactor was modelled with rigid material model in LS-DYNA (MAT20). Fig. 6 shows the FE mesh for the panel and impactor that was generated for this study based on the experiment setup (Choi and Chang 1992). To model appropriate contact algorithm between the impactor and the laminated composite plate, automatic surface to surface contact was used.

5. Results and discussion

As mentioned in the previous sections, the damage in a laminated panel can be divided into two main categories which are the main energy absorption mechanism for low velocity impact phenomenon. These two categories are discussed in this section and other obtained results were explained and compared to the experimental results.

5.1 Interlaminar failure

The results of the interlaminar failure for the panels discussed in this study are shown by Figs. 7-10. Figs. 7 and 8 show a peanut shape delamination that developed at the lower 0/90 and 45/-45 interfaces which oriented along the lower ply fibre direction of the interfaces. The delamination prediction was found to be in very good agreement with experiments for size, shape and orientation (Choi and Chang 1992). Simulation results also show a delamination that oriented itself
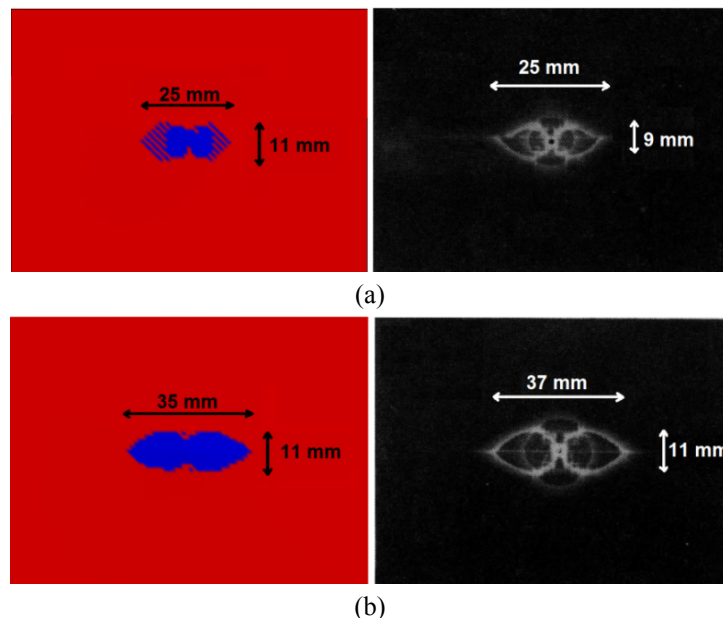

(a)

(b)

Fig. 7 Comparison between delamination shape obtained by simulation and experimental results from (Choi HY and Chang FK 1992) (lower 0/90 interface) for S1 specimen: (a) Velocity 4 m/s; (b) Velocity 6.7 m/s
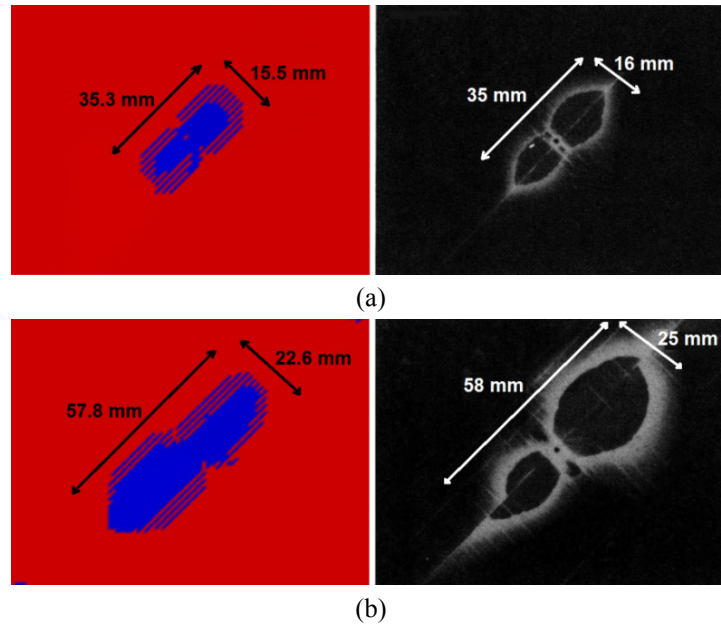
(a)

(b)

Fig. 8 Comparison between delamination shape obtained by simulation and experimental results from (Choi HY and Chang FK 1992) (lower -45/45 interface) for S2 specimen: (a) initial velocity: 5.89 m/s; (b) initial velocity: 9.02 m/s
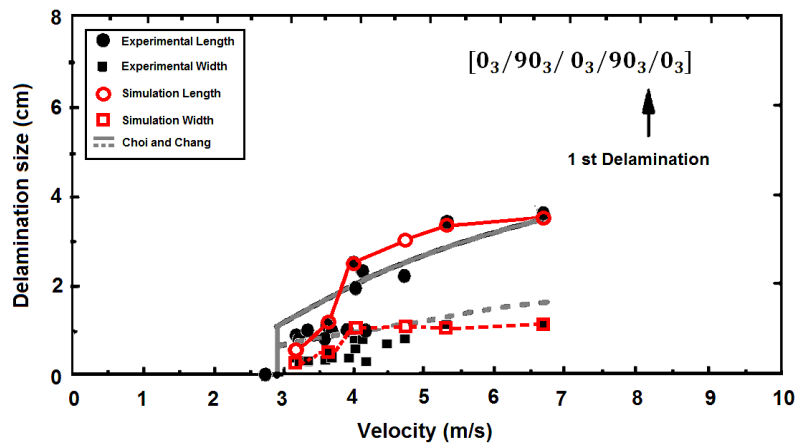

Fig. 9 Comparison between delamination size obtained by simulation, experimental data and results from the literature (Choi and Chang 1992) for S1 specimen

along the fibre direction of the bottom ply of the delaminated interface. Also comparison between delamination size obtained by simulation, experimental data and results from the literature (Choi and Chang 1992) can be seen in Figs. 9 and 10.

The growth of delamination areas versus time for both S1 and S2 specimens at the impact velocity of 6.7 m/s are shown by Fig. 11.
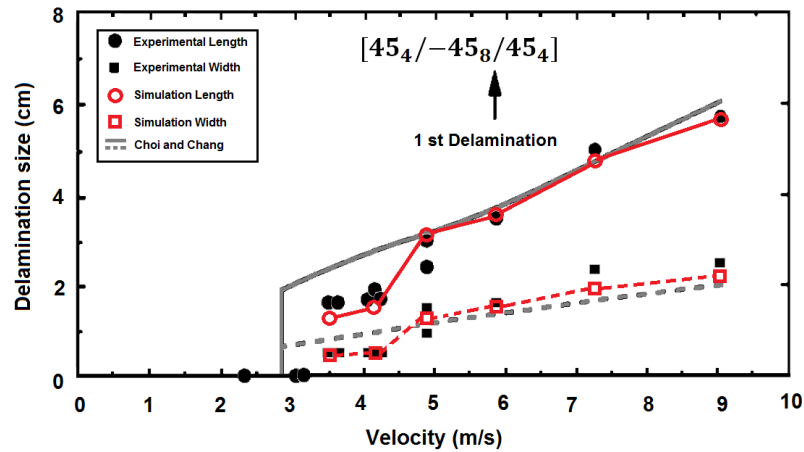
Fig. 10 Comparison between delamination size obtained by simulation, experimental data and results from the literature (Choi and Chang 1992) for S2 specimen
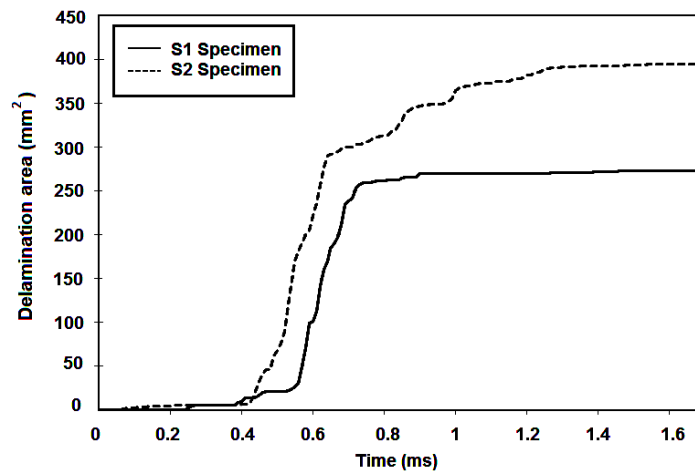

Fig. 11 Delamination areas versus time (ms) for impact velocity of 6.7 m/s found forS1 and S2 Specimens (lower inter-face)

5.2 Intralaminar failure (fibre/matrix failure)

Matrix cracks are the main energy absorbing mechanism in low velocity impact phenomenon for laminated composite structures. The intralaminar fibre and matrix damage could not be evaluated precisely by experiment (Choi and Chang 1992); however, it could be only studied by post processing the simulation results and plotting the history variables (HV) for the material model (MAT54). These variables are set between 0 and 1 based on failure modes in the lamina: fibre tensile mode (HV#1), fibre compressive mode (HV#2), matrix tensile mode (HV#3), and matrix compressive mode (HV#4).

The simulation results of the reference model show the intralaminar failure mode in matrix tensile failure (Figs. 12 and 13). The two-colored fringe plot of this failure variable for the
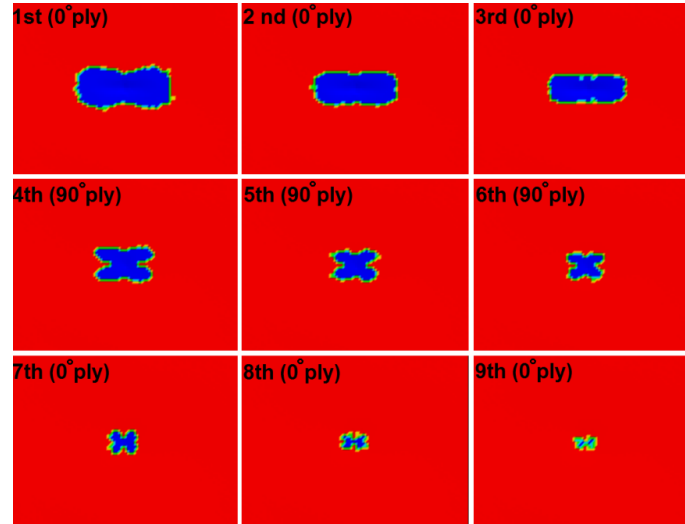
Fig. 12 Contour of tensile matrix mode failure (e_m) at different integration point in lower and upper Shell model at time (1.7 ms) for the initial impact velocity of 6.7 m/s for the S1 specimen
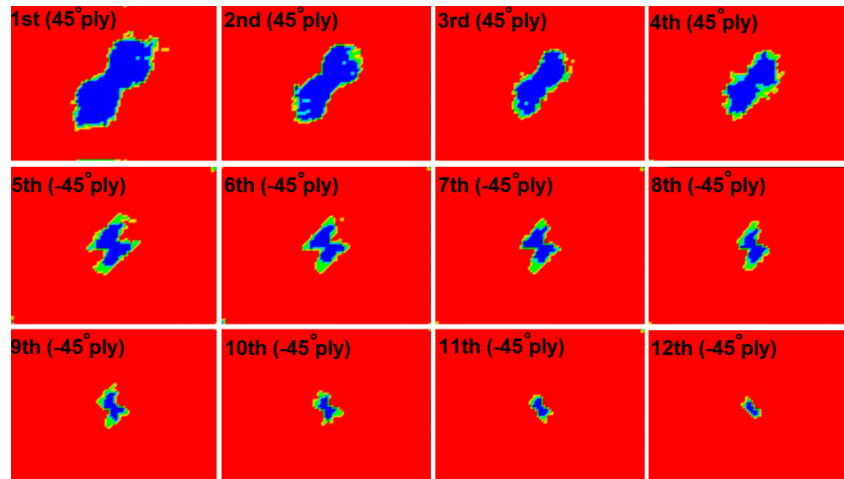

Fig. 13 Contour of tensile matrix mode failure (e_m) at different integration point in lower and upper Shell model at time (1.7 ms) for the initial impact velocity of 5.89 m/s for the S2 specimen

individual integration points across the thickness of the 9th bottom plies for S1 specimen and 12th bottom plies for S2 specimen are shown by these two pictures. Damage starts from the bottom plies on the opposite side of the impact surfaces. This region is in tension because of plate bending and the low tensile strength in the matrix direction (Y_t = 45 MPa); consequently the matrix failure in tensile mode is resulted. This phenomenon with higher damage in the bottom plies can be observed for 9th and 12th bottom plies as well as for each single shell element (3 and 4 integration points (IP) in lower shell element and 6 or 8 IP in upper shell element corresponding to each ply sequence).
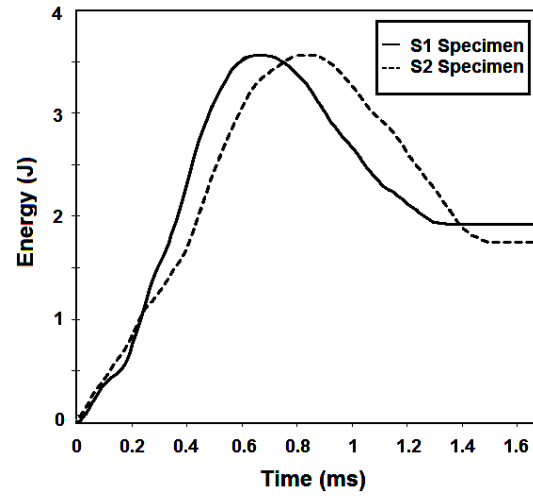
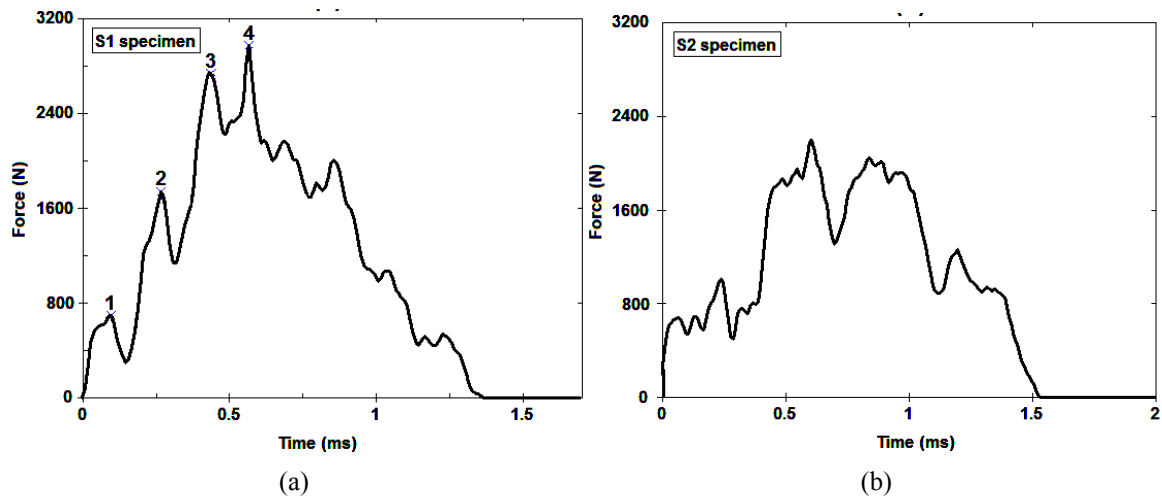Fig. 14 Energy plot for the impact velocity of 6.7 m/s for S1 and S2 specimens

| (a) | (b) |

Fig. 15 Contact force plotfor the initial impact velocity of 6.7 m/s for: (a) S1 specimen; and (b) S2 specimen

Fig. 14 shows the variation in the internal energy of the plate for S1 and S2 specimens, and shows the amount of the absorbed energy for these two specimens mainly due to intralaminar and interlaminar damages of the laminated plate.

5.3 Contact force of the impact

The numerical contact force can be plotted by recalculating the impactor's rigid body acceleration result versus impact time, and it is shown by Fig. 15(a) for the initial impact velocity of 6.7 m/s associated with $[0_3 / 90_3 / 0_3 / 90_3 / 0_3]$ ply sequence (Specimen S1). Also, Fig. 15(b) shows contact force plot for S2 specimen. Sudden drop in the force-time curve was expected due
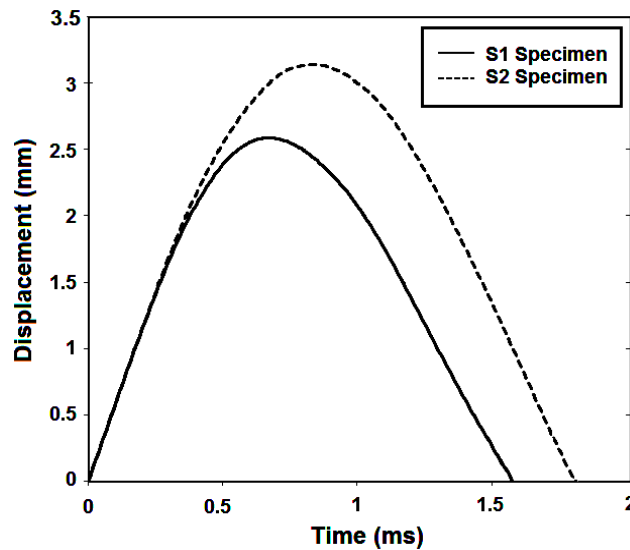
Fig. 16 Displacement versus time for S1 and S2 specimens under impact velocity of 6.7 m/s

to intralaminar and interlaminar failures of the structure which is represented correctly by the simulation. As Fig. 15(a) shows, four points on the force-time curve can be identified. Each point represents failures in the plate:

- Point 1 shows the intralaminar failure mode in matrix tensile failure of the 3th bottom plies (opposite side of the impact surface).
- Point 2 shows the intralaminar failure mode in matrix tensile failure of the 6th bottom plies.
- Point 3 shows the growth of intralaminar failure with higher rate.
- Point 4 shows the growth of delamination with high rate (as can be seen from Fig. 11) and matrix compressive failure of the 3th upper plies (impact surface).
- The further drops in the contact force plot are due to plate oscillation after impacting.

The displacement of the plate versus time is shown by Fig. 16. As both Figs. 15 and 16 demonstrate, the time duration for displacements and contact forces versus time are close to each other and address classification of this impact problem under low velocity impact (refer to Fig. 1(a)). Modelling parameters such as element formulation, number of cohesive zones and mesh size were explored for results accuracy and simulation time. Considering Belytschko-Tsay element formulation along with 1mm element size provided the best results which match the experimental observations. In addition, it was observed that increasing number of cohesive zones results unrealistic stiffness for the plate.

All the simulations were carried out by a PC with one 2.5 GHz Intel core i5 processor and 4 GB of RAM. Use of two shell elements with integration points for each single ply significantly decreases solution time to approximately 20 minutes. The results of the simulation demonstrates that shell elements with cohesive zone modelling have the potential to be adopted as an effective simulation tool to predict a complex impact-induced damage patterns in realistic laminated structures not only for research studies but also industrial applications.

6. Conclusions

In this paper, modelling of interalaminar and interlaminar failure modes in laminated composite were investigated by using a multi-layered shell element approach. The results showed a high level of accuracy, which was confirmed with the test results, in terms of size, shape and orientation of delaminated areas. According to the corresponding test report, the peanut shaped damage which represents delamination in each layer was correctly simulated for the size and orientation. Moreover, the major modelling parameters such as material model, number of cohesive zones, element formulation and element size have been found which result accuracy and stability for the simulation. According to our investigation, increasing the number of cohesive zones results in reduction in the stiffness of the laminated plate, and deviates the simulation results from reality. In addition, using element size equal to the specimen's thickness while considering Belytschko-Tsay as the element formulation leads to a better prediction of the delamination, with reduction in simulation time. This paper demonstrates an efficient approach to studying delamination in composite material by application of multi-layered shell element and cohesive zones. The approach uses a low complexity modelling procedure with high accuracy of results to study delamination in composite materials under low velocity impact.

References

Abrate, S. (1998), *Impact on Composite Structures*, University Press, Cambridge, UK.

Aymerich, F., Dore, F. and Priolo, P. (2008), "Prediction of impact-induced delamination in cross-ply composite lminates using cohesive interface elements", *Compos. Sci. Technol.*, **68**(12), 2383-2390.

Belytschko, T., Lin, J. and Tsay, C.S. (1984), "Explicit algorithms for nonlinear dynamics of shells", *Comp. Meth. Appl. Mech. Eng.*, **42**(2), 225-251.

Benzeggagh, M.L. and Kenane, M. (1996), "Measurement of mixed-mode delamination fracture toughness of unidirectional glass/epoxy composites with mixed-mode bending apparatus", *Compos. Sci. Technol.*, **56**(4), 439-449.

Chang, F.K. and Chang, K. (1987), "A progressive damage model for laminate composites containing stress concentrations", *J. Compos. Mater.*, **21**(9), 834-855.

Choi, H.Y. and Chang, F.K. (1992), "A model for predicting damage on graphite/epoxy laminated composites resulting from low-velocity point impact", *J. Compos. Mater.*, **26**(14), 2l34-2169.

Davies, G.A.O. and Olsson, R. (2004), "Impact on composite structures", *Aeronaut. J.*, **108**(1089), 541-563.

Davies, G.A.O. and Zhang, X. (1995), "Impact damage prediction in carbon composite structures", *Int. J. Impact Eng.*, **16**(1), 149-170.

Dogan, F., Hadavinia, H., Donchev, T. and Bhonge, P.S. (2012), "Delamination of impacted composite structures by cohesive zone interface elements and tiebreak contact", *Cent. Eur. J. Eng.*, **2**(4), 612-626

Feraboli, P., Wade, B., Deleo, F., Rassaian, M., Higgins, M. and Byar, A. (2011), "LS-DYNA MAT54 modelling of the axial crushing of a composite tape sinusoidal specimen", *Composites*: *Part A*, **42**(11), 1809-1825.

Finn, S.R. and Springer, G.S. (1993), "Delamination in composite plates under transverse static or impact loads –a model", *Compos Struct.*, **23**(3), 177-190.

Heimbs, S., Heller, S., Middendorf, P., Hahnel, F. and Weiße, J. (2009), "Low velocity impact on CFRP plates with compressive preload: Test and modelling", *Int. J. Impact Eng.*, **36**(10), 1182-1193.

Hosseini-Toudeshky, H., Hamidi, B., Mohammadi, B. and Oveysi, H.R. (2006), "Finite element based prediction of failure in laminated composite plates", *Fract. Nano Eng. Mater. Struct.*, *Proceedings of the 16th European Conference of Fracture*, Netherlands, July, pp. 311-312

Hosseini-Toudeshky, H., Saeed Goodarzi, M. and Mohammadi, B. (2013), "Prediction of through the width

Delamination growth in post- buckled Laminates under fatigue loading using de-cohesive law", *Struct. Eng. Mech.*, *Int. J.*, **48**(1), 41-56.

Jackson, P.A., Hunter, J. and Daly, M. (2012), "Jane's All the World's Aircraft 2012/2013", Jane's Information Group.

Kiani, M., Shiozaki, H. and Motoyama, K. (2013), *Composite Materials and Joining Technologies for Composites* (Volume 7), "Using experimental data to improve crash modeling for composite materials", *Proceedings of the 2012 Annual Conference on Experimental and Applied Mechanics*, pp. 215-226.

Kim, E.H., Rim, M.S., Lee, I. and Hwang, T.K. (2013), "Composite damage model based on continuum damage mechanics and low velocity impact analysis of composite plates", *Compos. Struct.*, **95**, 123-134.

LS-DYNA keyword user manual (2012), Version 971 R6.0.0, Vol. 1, February.

Maio, L., Monaco, E., Ricci, F. and Lecce, L. (2013), "Simulation of low velocity impact on composite laminates with progressive failure analysis", *Compos. Struct.*, **103**, 75-85.

Olsson, R. (2003), "Closed form prediction of peak load and delamination onset under small mass impact", *Compos. Struc.*, **59**(3), 341-349.

Reid, S.R. and Zhou, G. (2000), "Impact Behaviour of Fibre reinforced Composite Materials and Structures", CRC Press.

Schweizerhof, K., Weimar, K. and Rottner, T. (1998), "Crashworthiness analysis with enhanced composite material models in LSDYNA: Merits and limits", *Proceeding of Fifth LSDYNA International User Conference*, Livermore Software Technology Corp., Livermore, CA, USA, September.

Wade, B. and Feraboli, P. (2012), "Simulating laminated composites using LS-DYNA material model MAT54 part I: [0] and [90] ply single-element investigation", University of Washington.

Wang, J., Waas, A.M. and Wang, H. (2013), "Experimental and numerical study on the low-velocity impact behaviour of foam core sandwich panels", *Compos. Struct.*, **96**, 298-311.

Zheng, D. (2007), "Low velocity impact analysis of composite laminated plates", Ph.D. Dissertation, The Graduate Faculty of The University of Akron, OH, USA.

Zhou, J., Guan, Z.W. and Cantwell, W.J. (2013), "The impact response of graded foam sandwich structures", *Compos. Struct.*, **97**, 370-377.

CC